[9]Visser, K. D., Nelson, R. C., and Ng, T. T., "Method of Cold Smoke Generation for Vortex Core Tagging," *Journal of Aircraft*, Vol. 25, No. 11, 1988, pp. 1069–1071.

[10]Huang, X. Z., and Hanff, E. S., "Prediction of Leading-Edge Vortex Breakdown on a Delta Wing Oscillating in Roll," AIAA Paper 92-2677, June 1992.

[11]Ericsson, L. E., and Beyers, M. E., "Ground Facility Interference Effects on Slender Vehicle Dynamics," AIAA Paper 95-0795, 1995.

Application of Finite Strip Method to Composite Panel Flutter Analysis

L. C. Shiau* and S. T. Hwang†
National Cheng-Kung University, Tainan 70101, Taiwan, Republic of China

Introduction

COMPOSITE materials have been widely used in aeronautical industries to replace metals in the aircraft structures for the purpose of weight saving. Currently, in high-performance aircraft, composite materials are mostly used to make the skins of wings and fuselage of an aircraft. During high-speed flight, the external skin panel of an airframe may exhibit flutter. This type of aeroelastic instability has received much attention in the past 40 years.[1,2] Because the finite-element method (FEM) was first applied to panel flutter by Olson[3] in 1967, it has gained widespread attention by aeroelasticians, and many panel flutter analyses were done by using the FEM.[4,5] Although the FEM is the most powerful and versatile tool of solution in panel flutter analysis, it may be unnecessary for structures that have regular geometric plans and simple boundary conditions. Hence an alternative method that can reduce the computational effort, but at the same time, retain to some extent, the versatility of the finite-element analysis, is desirable. In this Note, the finite-strip method (FSM) developed by Cheung[6] in 1968 is applied to the flutter analysis of composite panels.

Equation Formulation

Consider a symmetric composite laminated thin plate with length a, width b, thickness h, and mass density per unit volume ρ, as shown in Fig. 1. The plate is assumed to consist of N layers of homogeneous anisotropic sheets bonded together. Supersonic airflow with air density ρ_a, flow velocity U_a, Mach number M_∞, and aerodynamic pressure Δp is assumed passing over the top surface of the plate with an angle Λ measured counterclockwise from the x axis.

The governing differential equation of motion for the plate can be obtained as

$$D_{11}\frac{\partial^4 w}{\partial x^4} + 4D_{16}\frac{\partial^4 w}{\partial x^3 \partial y} + 2(D_{12} + 2D_{66})\frac{\partial^4 w}{\partial x^2 \partial y^2} + 4D_{26}\frac{\partial^4 w}{\partial x \partial y^3} + D_{22}\frac{\partial^4 w}{\partial y^4} + \rho h \frac{\partial^2 w}{\partial t^2} + \Delta p = 0 \tag{1}$$

where w is the normal displacement of the plate. The flexural and torsional rigidities D_{ij} of the plate take the form of

$$D_{ij} = \frac{1}{3}\sum_{k=1}^{N}(\bar{Q}_{ij})_k\left(z_k^3 - z_{k-1}^3\right), \qquad (i, j = 1, 2, 6) \tag{2}$$

Received 17 October 1999; revision received 10 January 2000; accepted for publication 20 March 2000.

*Professor, Institute of Aeronautics and Astronautics; lcs@mail.iaa.ncku.edu.tw.

†Former Graduate Student, Institute of Aeronautics and Astronautics.

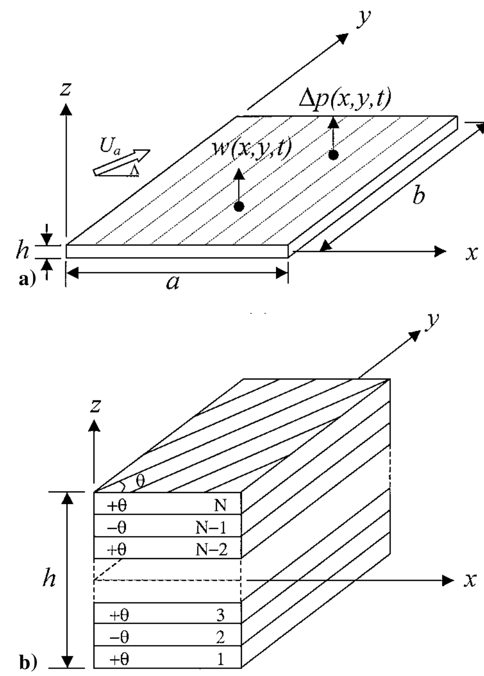

Fig. 1 a) Panel geometry and mesh divisions, and b) ply-stacking sequence.

where $(\bar{Q}_{ij})_k$ is the transformed reduced stiffness of the kth layer and z_k is defined in Fig. 1. The aerodynamic pressure Δp is approximated by quasi-steady aerodynamic theory as

$$\Delta p(x, y, t) = \frac{-\rho_a U_a^2}{(M_\infty - 1)^{\frac{1}{2}}}\left(\frac{\partial w}{\partial x}\cos\Lambda + \frac{\partial w}{\partial y}\sin\Lambda + \frac{1}{U_a}\frac{M_\infty^2 - 2}{M_\infty^2 - 1}\frac{\partial w}{\partial t}\right) \tag{3}$$

When the FSM is used for the analysis, the plate is divided into several strips, as shown in Fig. 1. The displacement function $w(x, y)$ for a strip is assumed as

$$w(x, y) = \sum_{m=1}^{r} f_m(x) Y_m(y) \tag{4}$$

where $f_m(x)$ is a polynomial function in the x direction and Y_m is a series that satisfies the end conditions in the y direction. For a strip with two nodal lines and 2 degrees of freedom at each nodal line, the polynomial function is identical to that for a beam element in the FEM. The series term $Y_m(y)$ for a plate with simply supported ends is taken as

$$Y_m(y) = \sin(m\pi y/a), \qquad m = 1, 2, 3, \ldots, r \tag{5}$$

Equation (4) can also be expressed in terms of the strip nodal line displacement $\{q_s\}$ as

$$w(x, y) = \sum_{m=1}^{r} Y_m \sum_{i=1}^{4}[B_i]_m\{q_i\}_m = \sum_{m=1}^{r}[S]_m\{q_s\}_m = [S]\{q_s\} \tag{6}$$

where B_i is the shape function associated with q_i and $\{q_s\}^T = \{w_1 \;\; \theta_1 \;\; w_2 \;\; \theta_2\}$.

On substitution of Eq. (6) into Eqs. (1) and (3), the bending stiffness $[k_s]$, mass $[m_s]$, aerodynamic damping $[A_{sd}]$, and aerodynamic force $[A_{sf}]$ matrices of the strip can be obtained as

$$[k_s] = \iint [G]^T[D][G]\,\mathrm{d}x\,\mathrm{d}y \tag{7}$$

$$[m_s] = \iint \rho h[S]^T[S]\,\mathrm{d}x\,\mathrm{d}y \tag{8}$$

$$[A_{sd}] = \iint [S]^T[S]\,\mathrm{d}x\,\mathrm{d}y \tag{9}$$

$$[A_{\mathrm{sf}}] = \iint [S]^T \left[\frac{\partial S}{\partial x}\right] \cos\Lambda \, \mathrm{d}x \, \mathrm{d}y + \iint [S]^T \left[\frac{\partial S}{\partial y}\right] \sin\Lambda \, \mathrm{d}x \, \mathrm{d}y \tag{10}$$

where the matrix

$$[G]^T = \left[\frac{\partial^2 S}{\partial x^2} \quad \frac{\partial^2 S}{\partial y^2} \quad 2\frac{\partial^2 S}{\partial x \partial y}\right]$$

is the strain-displacement relation matrix. Each strip has 4 degrees of freedom; hence the size of the above matrices will be $4m \times 4m$.

By assembling the strips for the entire plate system and applying the kinematic boundary conditions, we find that the equation of motion becomes

$$[M]\{\ddot{q}\} + \bar{g}[A_d]\{\dot{q}\} + \bar{\lambda}[A_f]\{q\} + [K]\{q\} = \{0\} \tag{11}$$

where $\bar{\lambda}$ is the aerodynamic pressure parameter and $\bar{g}$ is the aerodynamic damping parameter.

Assuming that the plate motion is an exponential function of time, i.e., $\{q\} = \{q\}e^{\nu t}$, where ν is the complex frequency of oscillation and introducing some nondimensional variables, we then find that the equation of motion becomes

$$([K] + \lambda[A_f] - k[M])\{q\} = \{0\} \tag{12}$$

The nondimensional parametes λ and k are defined as

$$\lambda = \bar{\lambda}a^3 \big/ D_{11}^{(0)}, \qquad k = -g(\nu/\omega_0) - (\nu/\omega_0)^2$$

$$g = \bar{g}/\rho h \omega_0, \qquad \omega_0^2 = D_{11}^{(0)} \big/ \rho h a^4$$

where $D_{11}^{(0)}$ is the value of D_{11} when all fibers are aligned with the x axis.

Equation (12) represents an eigenvalue problem. For zero flow velocity, $\lambda = 0$, the eigenvalues k are real. As the flow velocity increases from zero, two eigenvalues will usually approach each other and coalesce to k at a value of $\lambda = \lambda_{\mathrm{cr}}$, which is a critical value of dynamic pressure, and become complex-conjugate pairs for $\lambda > \lambda_{\mathrm{cr}}$.

Results and Discussion

First, a comparison of efficiency for the FSM and the FEM[7] is given in Table 1 for flutter analysis of a square isotropic panel with various cross-flow angles. All the analyses were performed on a personal computer with Pentium II 233 CPU, 96-MB RAM, WIN95 operating system, and MS FORTRAN PowerStation 4.0 compiler. With the same accuracy, the CPU time required for the FSM was less than $\frac{1}{3}$ of that for the FEM. Then, for the composite laminates, the panel considered for the analysis was a symmetric angle-ply laminate with simply supported edges. The material constants were $E_1 = 26.5E_2$, $G_{12} = G_{13} = G_{23} = 1.184E_2$, and $\nu_{12} = 0.21$. Three different meshes (4×4, 4×8, and 8×4) were used in the FSM to study the effects of the strip number (n) and series term (m) on accuracy of the solutions for the composite laminates. Results obtained for the plates were compared with results obtained with the FEM.[7] Figure 2 shows the effect of fiber orientation on the flutter boundaries for a square panel with three different cross-flow angles ($\Lambda = 0, 45, 90$ deg) and two different layer numbers ($N = 2, 10$). For a plate with only two layers, the bending–twisting stiffness terms not only have a destabilizing (or stabilizing) effect on the flutter boundary but also affect the accuracy of the FSM results. When compared with the FEM results, the 4×4 mesh give satisfactory results for almost all cases except for the laminates with $N = 2$, $\Lambda = 90$ deg, and a fiber angle between 50 and 70 deg. If the strip number is increased from 4 to 8 (i.e., the 8×4 mesh), the accuracy of the results is not improved. However, the accuracy can be improved by increasing the series term. The 4×8 mesh gives good results for all cases shown in Fig. 2. Figure 3 shows the flutter boundaries as a function of fiber orientation for a rectangular angle-ply laminated plate with a length/width ratio of 2.0. For both $\Lambda = 0$ and 45 deg flow angles, it is seen that the FSMs with 4×4 and 8×4 meshes give unsatisfactory results for a plate with $N = 2$ and a fiber angle between 30 and 70 deg. The 4×8 mesh gives only acceptable results. Increasing the series terms will improve the results.

Table 1 Flutter boundaries for a square isotropic plate by the FSM

Mesh	$\Lambda = 0$ deg		$\Lambda = 45$ deg		$\Lambda = 90$ deg	
$n \times m$	CPU, s	λ_{cr}	CPU, s	λ_{cr}	CPU, s	λ_{cr}
4×4	0.44	508.6	0.88	524.4	0.88	505.1
4×6	1.10	508.6	2.64	525.9	2.64	511.9
4×8	2.19	508.6	6.32	526.1	5.93	512.5
6×4	1.15	511.9	2.37	524.5	2.19	505.1
6×6	3.24	511.9	9.11	526.1	8.13	511.9
6×8	6.43	511.9	16.91	526.2	19.06	512.5
8×4	3.24	512.4	6.09	524.5	5.61	505.1
8×6	8.24	512.4	18.07	526.1	18.67	511.9
8×8	18.51	512.4	43.89	526.2	43.72	512.5
FEM (4×4)	10.93	512.2	12.47	525.8	10.93	512.2
FEM (5×5)	43.06	512.5	43.45	526.2	43.06	512.5
Exact	——	512.6	——	——	——	512.6

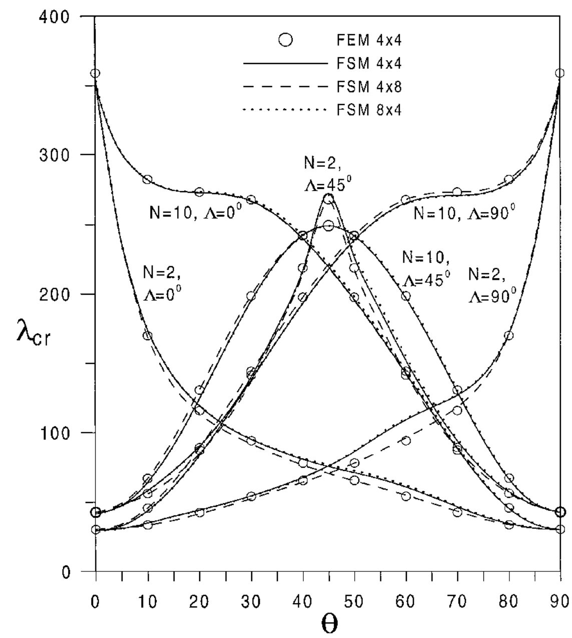

Fig. 2 Flutter boundaries for graphite-epoxy plate with *a*/*b* = 1.0.

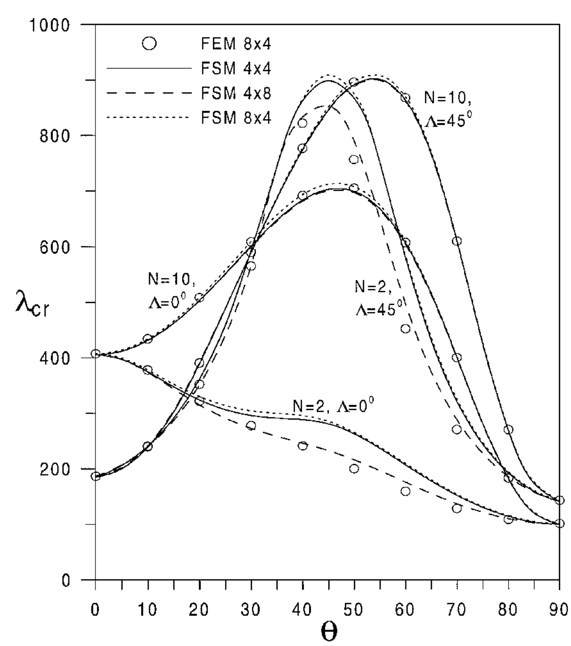

Fig. 3 Flutter boundaries for graphite-epoxy plate with *a*/*b* = 2.0.

Conclusions

The application of the finite strip method to supersonic flutter of composite laminated panels has been presented. The present formulations are for symmetric laminates but it is easy to extend the formulations to general laminated plates. Based on the present results, the following conclusions can be made:

1) For isotropic panels, the number of strips and series terms that required giving satisfactory results by the finite strip method is dependent on the flow angularity.

2) When fiber orientation is not aligned with the x- or y-direction, increasing series terms will rapidly improve the accuracy of the results.

3) Flutter boundary (λ_{cr}) is independent of the series terms when the airflow is along the x-direction ($\Lambda = 0°$) and is independent of the strip numbers when the airflow is along y-direction ($\Lambda = 90°$).

References

[1]Ventres, C. S., and Dowell, E. H., "Comparison of Theory and Experiment for Nonlinear Fluttering of Loaded Plates," *AIAA Journal*, Vol. 8, No. 11, 1970, pp. 2022–2030.

[2]Shiau, L. C., "Flutter of Composite Laminated Beam Plates with Delamination," *AIAA Journal*, Vol. 30, No. 10, 1992, pp. 2504–2511.

[3]Olson, M. D., "Finite Element Applied to Panel Flutter," *AIAA Journal*, Vol. 5, No. 2, 1967, pp. 2267–2270.

[4]Yang, T. Y., "Flutter of Flat Finite Element Panels in a Supersonic Potential Flow," *AIAA Journal*, Vol. 13, No. 11, 1975, pp. 1502–1507.

[5]Shiau, L. C., and Chang, J. T., "Transverse Shear Effect on Flutter of Composite Panels," *Journal of Aerospace Engineering*, Vol. 5, No. 4, 1990, pp. 465–479.

[6]Cheung, Y. K., *Finite Strip Method in Structural Analysis*, Pergamon, New York, 1976, pp. 27–34.

[7]Wu, T. Y., "Geometrically Nonlinear Analysis of Laminated Plates by Finite Element Method," Ph.D. Dissertation, Inst. of Aeronautics and Astronautics, National Cheng-Kung Univ., Taiwan, 1995.

Bounded-Variable Gauss–Newton Algorithm for Aircraft Parameter Estimation

R. V. Jategaonkar*
DLR, German Aerospace Research Center, 38108 Braunschweig, Germany

Introduction

ESTIMATION of stability and control derivatives or of nonlinear unsteady aerodynamic effects from flight data is a subject of continuous interest. The time-domain approach based on the output error method is widely used for this purpose.[1–3] It leads to a nonlinear optimization problem, which is solved mostly using the unconstrained Gauss–Newton method. Parameter estimation subject to simple bounds can, however, be relevant in some cases. Two typical applications are the following: 1) parameters that describe the physical effects, in the present case aerodynamic effects, are often constrained to lie in a certain range, for example, the Oswald's factor[4] characterizing the increase in drag over ideal condition caused by nonelliptical lift distribution and interference is typically limited to less than one or the time delay is always positive and hence greater than zero; and 2) estimation of highly nonlinear model parameters such as friction, which may lead to numerical difficulties caused by different reasons like poor guess of initial values.[5] Incorporation of such lower and upper bounds in aircraft parameter estimation using the Gauss–Newton method has not been hitherto reported in the literature. This Note, therefore, addresses the issues pertaining to extending the Gauss–Newton method to account for simple bounds and also demonstrates that the active-set strategy provides an efficient solution retaining the desirable properties of the Gauss–Newton method, namely, quadratic convergence and availability of statistical information regarding the accuracy of the estimates.

Received 20 November 1999; revision received 5 January 2000; accepted for publication 24 January 2000.

*Senior Scientist, Institute of Flight Research, Lilienthalplatz 7. Senior Member AIAA.

Problem Formulation

In the general case a dynamic system is represented as

$$\dot{x}(t) = f[x(t), u(t), \lambda] \qquad x(t_0) = x_0 \tag{1}$$

$$y(t) = g[x(t), u(t), \lambda] \tag{2}$$

$$z(t_k) = y(t_k) + v(t_k) \qquad k = 1, 2, 3, \ldots, N \tag{3}$$

where x is the n-dimensional state vector, y the m-dimensional observation vector, and u the p-dimensional control input vector. The system functions f and g are general nonlinear real valued vector functions. The measurement vector z is sampled at N discrete time points t_k, and the noise vector v is assumed to be a sequence of independent Gaussian random variables with zero mean and covariance matrix R. It is required to estimate the unknown system parameters λ and the initial conditions x_0 as well as the measurement noise covariance matrix R.

Unconstrained Gauss–Newton Method

The maximum likelihood estimates of the unknown parameters and of the unknown noise covariance matrix are obtained by minimizing the cost function[3,6]:

$$J(\Theta, R) = \frac{1}{2}\sum_{k=1}^{N}[z(t_k) - y(t_k)]^T R^{-1}[z(t_k) - y(t_k)]^T + \frac{N}{2}\ln|R| \tag{4}$$

where $\Theta = [\lambda^T, x_0^T]^T$ denotes the q-dimensional vector of unknown parameters, which may be extended to include bias errors in the measurements of response and control input variables.[6] Optimization of Eq. (4) is carried out in two steps. In the first step it can be shown that for any given value of Θ the maximum likelihood estimate of R is given by

$$\hat{R} = \frac{1}{N}\sum_{k=1}^{N}[z(t_k) - y(t_k)][z(t_k) - y(t_k)]^T \tag{5}$$

Having obtained an estimate of R, any optimization method can be applied to update the parameter vector Θ. The investigations in the past have, however, demonstrated that the derivative-free search methods such as Powell and downhill Simplex methods[7] or Extrem[8] and routinely available gradient-based methods such as quasi-Newton, conjugate-gradient, or Broyden-Fletcher-Goldfarb-Shanno (BFGS) algorithms[7] are much slower compared to the Gauss–Newton method, particularly for estimation involving large dynamic systems where the computational effort to compute the system responses and their gradients is high.[9,10] For aircraft parameter estimation purposes the Gauss–Newton method is therefore widely used.[1–3] The unconstrained Gauss–Newton method yields the iterative parameter update:

$$\Theta_{i+1} = \Theta_i + \Delta\Theta \quad \text{with} \quad \Delta\Theta = -F^{-1}G \tag{6}$$

where the $q \times q$ dimensional information matrix F and the q-dimensional gradient vector G are given by

$$F = \frac{\partial^2 J}{\partial \Theta^2} \approx \sum_{k=1}^{N}\left[\frac{\partial y(t_k)}{\partial \Theta}\right]^T R^{-1}\left[\frac{\partial y(t_k)}{\partial \Theta}\right] \tag{7}$$

$$G = \frac{\partial J}{\partial \Theta} = \sum_{k=1}^{N}\left[\frac{\partial y(t_k)}{\partial \Theta}\right]^T R^{-1}[z(t_k) - y(t_k)] \tag{8}$$